JP2.4

RETRIEVAL OF CLOUD OPTICAL PROPERTIES FROM INFRARED HYPER-SPECTRAL MEASUREMENTS: A NEW METHODOLOGY BASED ON LINE-BY-LINE MULTIPLE SCATTERING CODE AND MEASURED PARTICLES SIZE DISTRIBUTIONS

Tiziano Maestri, Robert E. Holz, and Paolo Antonelli

SSEC-Space Science and Engineering Center, University of Madison-Wisconsin, 1225 West Dayton Street, 53706, Madison, WI (USA)

1. ABSTRACT

A new methodology to retrieve cloud optical properties using hyper-spectral infrared measurements is presented. The new method makes use of line by line multiple scattering (LbLMS) simulations to retrieve spectrally resolved cloud optical depths from spectral radiance data. The retrieval requires knowledge of the clear sky profile and cloud boundaries. The cloud microphysical properties are retrieved by comparing the infrared spectral optical depths with a pre-computed optical depth database. This reference database is generated from an ensemble of measured cloud particle size distributions (PSD) and pre-computed single scattering and single particle optical properties for a variety of ice crystal habits.

The full methodology was applied to aircraft (Scanning High-resolution Interferometer Sounder, S-HIS), satellite (Atmospheric Infrared Sounder, AIRS) and ground based (Atmospheric Emitted Radiance Interferometer, AERI) hyper-spectral measurements collected during the Mixed Phase Artic Cloud Experiment (MPACE) 2004 in the North Slope of Alaska. Collocated lidar and radar measurements were used to validate the retrieval results.

2. INTRODUCTION

Operational atmospheric properties retrievals from satellite measurements are typically applied to only clear sky fields of view due to the complexity of assimilating cloudy radiances in to the NWP models. By not using cloudy radiances most of the data is not assimilated.

New methodologies for retrieving cloud properties from spectral infrared data have been developed recently ([Li et al., 2005], [Turner, 2005], [DeSlover et al., 1999]) but these retrievals are not operational. Nonetheless high spectral resolution satellite data offer an opportunity to improve our knowledge about clouds and then climate impact. The retrieval of cloud microphysical and optical properties from passive remote sensor is complicated by a variety of factors including technical, theoretical limitations and large uncertainties in the a-priori knowledge of the system under study. Infrared retrievals have been combined with techniques using the shortwave part of the spectrum ([Khokanovsky and Nauss, 2005], [Min and Duan, 2005]). Of course this requirement makes the technique available only in presence of scattered solar radiation.

Most retrieval methods are based on a simplified assumption of the cloud geometry with a focus on water droplets. The new technique presented in this paper characterizes the full geometrical thickness of the cloud layer and can be applied to water or ice clouds with different crystal shapes. Moreover, the most important feature of the new retrieval code is that the algorithm is designed to work with multiple sensors and perspectives (satellite, airborne or ground-base sensors). This makes the methodology suitable for intercomparisons using remote sensing instrumentations on different platforms.

3. FIELD EXPERIMENT AND INSTRUMENTS

The Mixed Phase Artic Cloud Experiment (MPACE) was conducted in Alaska (Barrow) between September and October 2004 and was funded by DOE-ARM. Three different infrared sensors have been considered in this study: the ground base interferometer AERI (Atmospheric Emitted Radiance

*Corresponding author address: Tiziano Maestri, SSEC, UW-Madison, 1225 West Dayton St., Madison, WI 53706; Fax: 608-262-5974; e-mail: tiziano@ssec.wisc.edu

Interferometer), the airborne interferometer S-HIS (Scanning High-resolution Interferometer Sounder) and the satellite based AIRS (Atmospheric Infra-Red Sounder).

The AERI spectral measurement range is 520-3300 cm^{-1} with a (apodized) spectral resolution of 0.5 cm^{-1}. The instrument field of view (FOV) is 1.3 degrees. During the MPACE experiment the instrument was operated in a rapid sampling mode with sky radiance spectrum measured every 20 seconds with periodic gaps for calibration. The absolute accuracy is better than 1% of the ambient radiance [Knuteson et al., 2004].

S-HIS is an aircraft scanning interferometer with similar specifications to AERI (design, spectral range, spectral resolution and accuracy), but a different FOV: 2 km at nadir when flying at 20 km of altitude. It was flying on-board the NASA Proteus at around 12.5 km of altitude [Revercomb et al., 1998].

AIRS is a high spectral resolution array grating spectrometer with a spectral coverage from 3.7 to 15.4 microns and a spectral response resolving power ($\lambda/\Delta\lambda$) of 1200. The infrared nadir spatial resolution is 13.5 km. Radiometric calibration is 3% [Aumann and Miller, 1995].

Cloud optical depths retrieved from the infrared measurements are validated using the Arctic High Spectral Resolution Lidar (AHSRL). The AHSRL is a multi-channel lidar capable of independent measurements of the cloud depolarization, extinction, and backscatter cross-section [Pironen and Eloranta, 1994]. The AHSRL measures two signals that can be processed to yield separate lidar returns from aerosol and molecular scattering. The separation is possible because the wavelength spectrum of the molecular lidar return is Doppler broadened by molecular thermal motion. The separation of molecular and aerosol returns permits the AHSRL to measure the extinction and aerosol backscatter cross-sections independently. The AHSRL also provides circular particulate depolarization measurements allowing for discrimination between ice and water. The laser wavelength is 0.532 micron and the altitude resolution is 7.5 m.

The Proteus (carrying the S-HIS) flight tracks near Barrow (where the AERI and the AHSRL are based) are presented in Figure 1. An AQUA overpass occurred at 22:23 local.

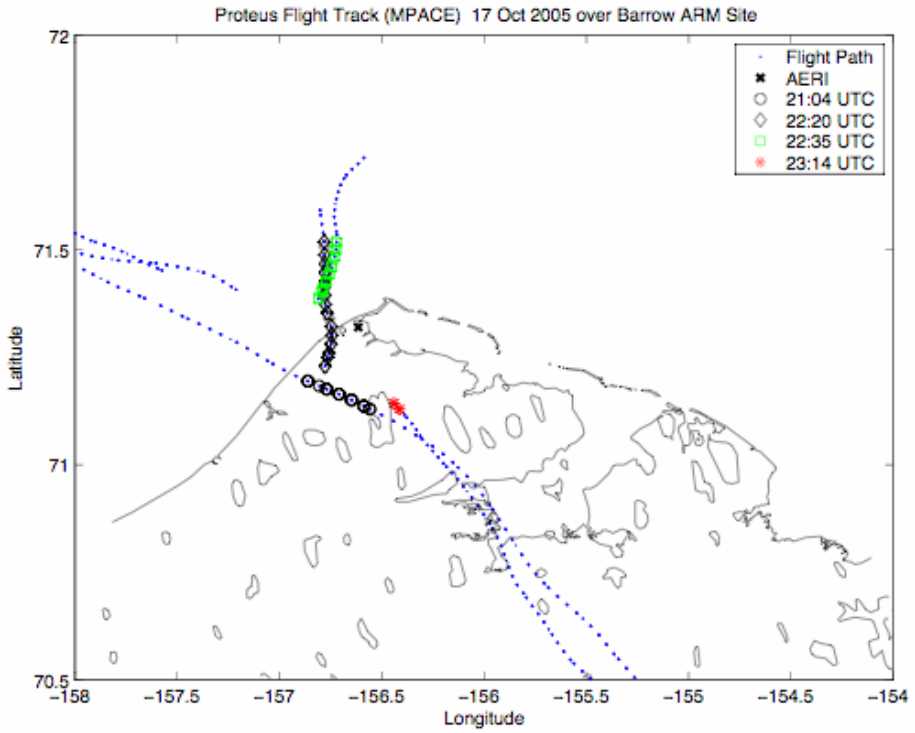

Figure 1: map of the Proteus flight track (blue dots) near Barrow ARM site (black x). The closest nadir S-HIS field of views are highlighted in black red or green.

4. RETRIEVAL METHODOLOGY

The presented retrieval scheme uses the LbLMS radiative transfer code, RTX, which is exploited to solve the radiative transfer equation for scattering layers and is based on a doubling and adding method. A description of the forward model can be found in Evans and Stephens [1991] and in a paper by Rizzi et al. [2002].

The retrieval methodology requires a-priori information of the clear sky and the cloud geometrical boundaries. Temperature and water vapor profiles are required as inputs in the code sequence. A simple code to exploit the ECMWF re-analysis grib files has been written and implemented into the retrieval code. The atmospheric profile is utilized to calculate the spectral gaseous optical depths. In this paper lidar measurements have been used to define the cloud boundaries. Without the lidar cloud boundaries an infrared cloud height retrieval can be used.

Local thermodynamic equilibrium and a plane parallel geometry of the cloud layers are assumed in the retrieval code. The code also assumes that the cloud optical depth is homogeneous. Nevertheless, the cloud can be divided in multiple layers and a temperature structure can be defined and resolved during the computations.

The gaseous optical depths (OD) are calculated using LbLRTM (version 9.4) [Clough and Iacono, 1995]. The spectroscopic gas features are taken from the Hitran 2004 database [Rothman at al., 2005]. Continuum absorption from 6 different gas types is also accounted for including the cross sections for the main CFCs gas types.

Once the layers' gaseous OD are computed, the layer to space (or ground when up-looking) transmittances are calculated and then convolved with the instrument spectral response function. Layer optical depths at the instrumental spectral resolution are then used as input in the retrieval code (RT-RET) together with the cloudy spectral measurements and input parameters.

RT-RET works sequentially on a defined wave-number array. It retrieves the cloudy spectral optical depths selected to resolve the cloudy spectral features. Channels are selected based on the instrument characteristics to optimize the sensitivity to the cloud microphysical spectral features in the 800-1000 cm^{-1} spectral range. RT-RET determines (for every wave-number) the optimal value of optical depth that the forward model requires to best fit the simulated radiance with the cloudy sky measurements. The first guess optical depth value is modified until the solution of the radiative transfer equation converges to the measured radiances. The user can choose how close the simulation has to be to the measured radiance data. Usually this threshold value is set so the simulation matches the measurements to within 0.5%.

Cloud microphysical features (particles size distribution and crystal habits) are indirectly accounted for into the code through a first guess assumption. The code is relativity independent of microphysical characteristics except for a first guess assumption of the spectral single scattering properties of the PSD: single scattering albedo, ϖ, and asymmetry parameter, g. These two spectral quantities are used to define the quantity of energy involved in the scattering processes and built up a simplified phase function (Henyey-Greenstein). These assumptions have negligible influence on the final results.

It is important to emphasize that the Henyey-Greenstein phase function accurately represents the scattering processes in the infrared, especially in the window 800-1000 cm^{-1} where the absorption coefficient is large and scattering can be considered a second order process, independent of the crystal shape and habit assumed. The radiance pattern in the 800-1000 cm^{-1} window is, in fact, strongly driven by the absorption processes that mainly contribute to define the characteristic slope of the brightness temperature in the band. It turns out that, independently of the first guess assumption on the scattering properties, the retrieved absorption optical depth results extremely precise in this band.

The first guess optical properties are then used to simulate the scattering processes and represent a simplified modeling of a second order process (with respect to absorption). In situ measurements and climatology can be used to improve the determination of the first guess scattering properties. Finally it can be demonstrated that the final results (optical depth and effective diameter), obtained after running a second iteration, are independent of the first guess scattering properties.

Spectral ODs are retrieved sequentially from the first to the last input wave-number. To speed up the computations, the optical depth

at the wave-number (i)th is initialized with the OD found for the wave-number (i-1)th. For down-looking and up-looking sensors a convergence algorithm defined by equations 1 and 2, are used to make the first guess OD converge to the final solution. This method has been found to be extremely efficient and only a few iterations (generally 3-4 maximum) are necessary to obtain a result with a precision higher then 0.5%.

Down-looking:

$$\Delta OD = \frac{\Delta R}{(F_s - F_c)\cdot t_c} \quad \text{(eq. 1)}$$

from the first order assumption:

$$R \approx t_c \cdot (\varepsilon_s F_s) + (1 - t_c)\cdot F_c$$

Up-looking:

$$\Delta OD = \frac{\Delta R}{(-F_c)\cdot t_c} \quad \text{(eq. 2)}$$

from the first order assumption:

$$R \approx (1 - t_c)\cdot F_c$$

where

t_c = cloud transmissivity
R = *measured radiance*
F_c = *cloud radiance*
F_s = *surface radiance*
ε_s = *surface emissivity (assumed 1)*

The retrieved infrared OD can be converted to shortwave values once the best PSD has been identified (after the second iteration of the code). The comparison is done with a pre-computed database of optical depths. Such comparison is performed on the slope of the retrieved absorption OD. The slopes of absorption ODs have been pre-computed for a subset of PSDs representative of different effective radii.

The database has been created using the Ping Yang single particle and single scattering properties (7 different habits are assumed) [Yang et al., 2005]. These optical properties have been used to compute the spectral optical feature (extinction coefficient, scattering coefficient, asymmetry parameter and Legendre coefficient of the exact phase function) for a large subset of PSDs derived from the Andy Heymsfield database of modified gamma type PSDs ([Baum et al., 2005], [Heymsfield et al., 2004]). The PSDs have been obtained from fitting theoretical gamma size PSDs to measured data collected in 6 different field experiments by various sensors.

Once a best fit is reached in the absorption OD comparison, then a best PSD and effective dimension representing the retrieved quantities is defined. A second iteration can be performed using the identified PSD scattering properties as new first guess. In this way the final retrieval of the spectral OD is refined. The effective dimension retrieval is, on the other hand, almost independent from the first guess assumption for the reasons explained above.

5. RESULTS

The Barrow Alaska 17th October 2004 cirrus case will be used to investigate the retrieval. This day is characterized by a geometrically thick cirrus cloud for most of the day.

Figure 2 presents the aerosol backscattering cross section in the upper panel and the circular depolarization ratio in the lower panel as measured by the AHSRL. Cloud base altitude varies from 4 to 7 km while the cloud top is more stable between 10 and 11 km. Backscattering coefficient cross section also gives an idea of the distribution of ice matter inside the cloud. It can be noted that cloud is optically homogeneous after 22:00. On the other hand in the time period ranging from 17:00 to 22:00 the lower cloud layers seem optically thicker than those close to the top. An optically thin particles layer is also present at an altitude of around 3 km. Its optical thickness is mostly negligible except during two short times periods: the first at around 18:00 and a second one at around 20:00. At these times a tenuous water cloud is formed as can be seen from the depolarization ratio values in Figure 2.

Cloud lidar retrieved optical depths are plotted in Figure 3 (black line). Optical depth is varying in time from values at around 0.2 to values larger than 2. Results from the retrieval code are also reported in the same figure. Optical depths are retrieved for all the 3 infrared sensors mentioned before. The retrieval was performed on a cloud filled AIRS field of view (green dot in Figure 3) as determined by the co-located MODIS brightness temperatures that show a cloudy uniform scene in the AIRS FOV. Comparisons between lidar measured OD and retrieved AIRS OD is difficult because of the different FOV of the instruments, nonetheless the result

is consistent with the lidar data. As far as it concerns S-HIS data (blue circles) the comparison is limited by the spatial offset with the lidar. In fact, the Proteus was not allowed to flight over the lidar site resulting in a spatial offset when compared to the AHSRL measurements. The S-HIS analyzed data correspond to FOVs that are at around 4 km far from the lidar location.

The retrieval algorithm was applied to up-looking AERI measurements. The AERI was located within the ARM facility next to the AHSRL. Close agreement between the AERI and AHSRL retrieved optical depths is then expected. The red circles in Figure 3 present the AERI retrieved ODs. The agreement is best after 21h30m, where relative differences are less than few percent. Before 21:30 UTC the infrared retrieved OD follows the pattern of the lidar measured ODs, but a time dependent overestimation is noted.

A possible explanation of why larger values are found for the infrared retrievals lies in the assumption of a homogeneous optical depth in the cloud thickness. An ideal experiment has been simulated in which the same value of OD (2 in the example of Figure 4) is assumed to be homogeneous or non-homogeneous in the cloud layer. In the second case, non-homogeneous, the optical depth of the cloud is assumed to be mostly due to ice in the lower layers. It can be noted that, given this configuration (represented in the left side of Figure 2), the infrared radiance values arriving at the ground-based detector are higher with respect to the homogenous case. This is strictly related with the fact that the mean emission temperature of the cloud has, in the non-homogeneous case considered, moved towards lower altitudes and then higher temperatures. Nonetheless, the retrieval code is in both cases assuming a uniformly distributed OD. For this example assume a uniform cloud extinction profile results in an over estimate of the actual cloud OD.

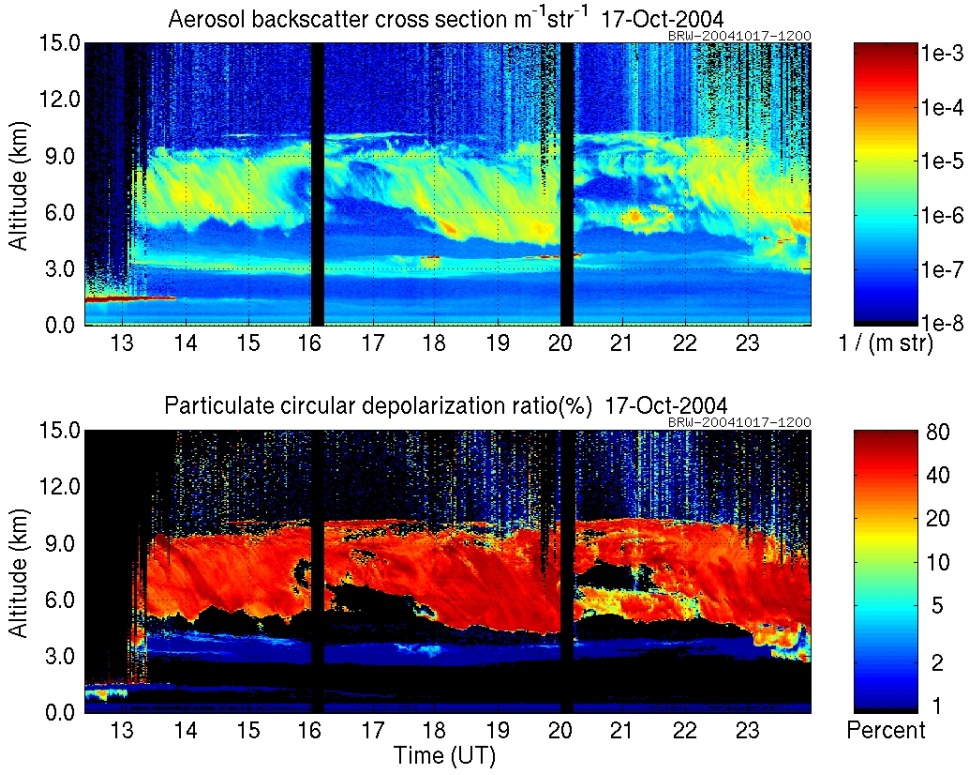

Figure 2: Backscattering cross section (upper panel) and depolarization ratio (lower panel) measured by the AHSRL during the second part of the day of the 17th October 2004. The lidar site location is Barrow, North of Alaska (USA).

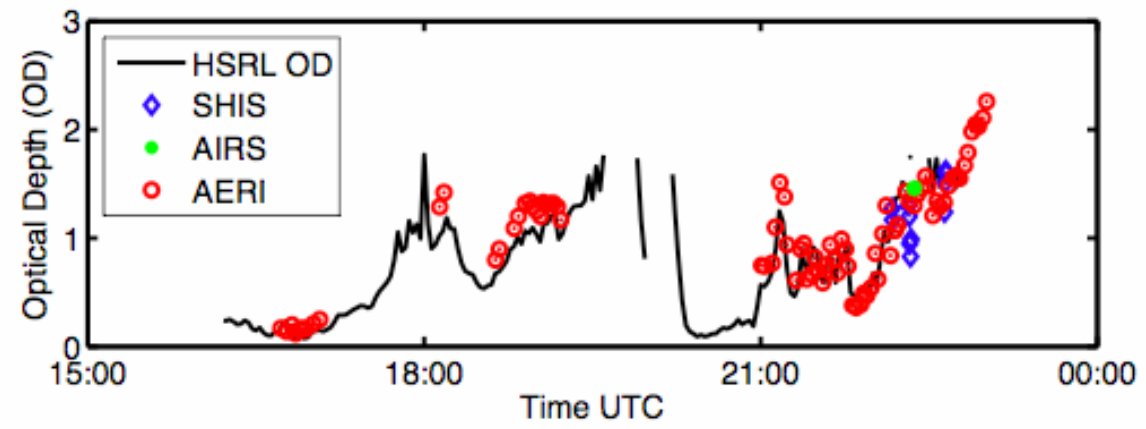

Figure 3: AHSRL measured cloud OD are compared to the retrieved values from the infrared sensors: AIRS, airborne S-HIS and ground based AERI.

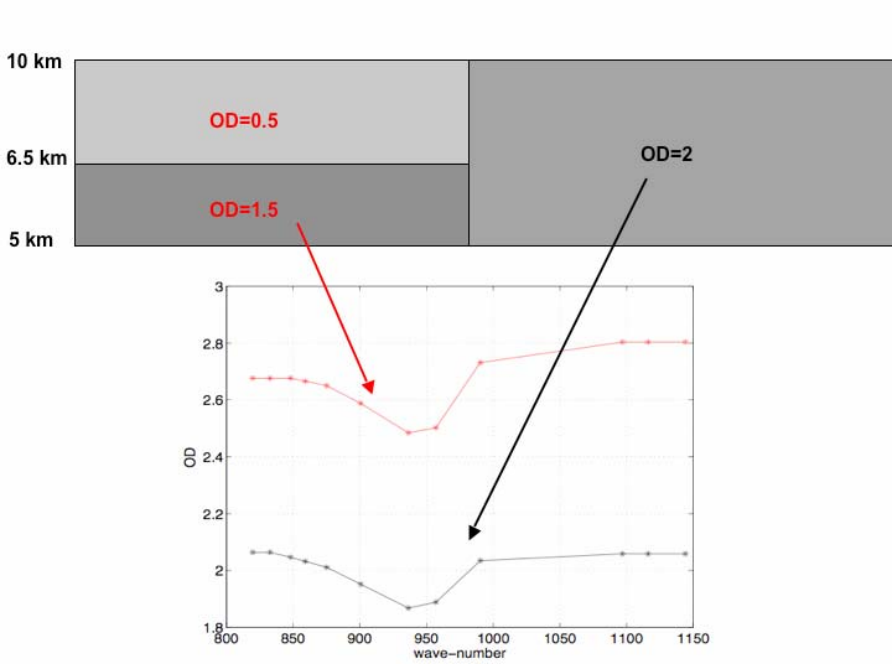

Figure 4: The AERI retrieved spectral optical depths are presented for a simulated 5km thick uniform cloud extinction profile (black) and a cloud with an identical total cloud optical depth but with the non-uniform extinction profile (red).

6. CONCLUSIONS

A new methodology for retrieving cloud optical properties from hyper-spectral infrared measurements has been presented. In summary the new features of this retrieval method with respect to other retrieval codes are that:

1) The retrieval works in optical depth space. The code algorithm and the pre-computed optical depth database are completely independent. This allows the possibility to expand and change the pre-computed ODs database without changing the retrieval algorithm and vice-versa. In addition, the second iteration can be performed at a later time with respect to a first retrieval iteration.
2) The code works using a simplified phase function, but the treatment of the scattering processes remains rigorous. This makes the scattering simplification less dependent on the

cloud configuration with respect other methods that use a scattering parameterization or a single scattering assumption. Some current methodologies are totally ignoring infrared scattering processes.

3) The same retrieval method can be applied to different hyper-spectral sensors. This allows consistent comparison which is advantageous for validation experiments. The algorithm is not only flexible on the type of instrument but also for the kind of platform used. It can be used for down or up- looking sensors and in theory applicable to every zenith angles

Retrieval results from the MPACE field experiment have been shown for infrared sensors (AERI, S-HIS and AIRS) on different platform (ground-based, airborne, satellite borne). Validation of the retrieved OD was performed by comparing AERI retrievals with co-located and time coincident AHSRL lidar measurements. Results show excellent agreement between the measured lidar data and the retrieved infrared OD. Some overestimations in the AERI retrieved ODs have been noticed for the first part of the day. The overestimations with respect to the lidar values could be explained using simulations and related to the assumption of a uniform OD distribution inside the cloud thickness.

Together with the OD retrieval a simultaneous retrieval of PSD/effective dimensions has been performed. Based on in situ measurements we have assumed that the ice crystals habit is bullet rosettes. Results have not been shown in this work since they are habit dependent and no validation was available for bullet rosettes.

7. REFERENCES

Aumann, H. H., and C. Miller, 1995: Atmospheric Infrared Sounder (AIRS) on the Earth Observing System. *SPIE*, **2583**, 32-343.

Baum B. A., A. J. Heymsfield, P. Yang, and S. Bedka, 2005: Bulk scattering properties for the remote sensing of ice clouds. Part I: Microphysical data and models*. J. Appl. Meteor.*, **44**, 1885-1895.

Clough, S. A., and M. J. Iacono, 1995: Line-by-line calculations of atmospheric fluxes and cooling rates II: Application to carbon dioxide, ozone, methane, nitrous oxide, and the halocarbons. *J. Geophys. Res*., **100**, 16,519-16,535.

DeSlover, D. H., W. L. Smith, P. K. Piironen, and E. W. Eloranta, 1999: A methodology for measuring cirrus cloud visible to infrared optical depth ratios. *J. Atmos. Oceanic Technol*., **16**, 251-262.

Evans, K., and G. Stephens, 1991: A new polarized atmospheric radiative transfer model. *J. Quant. Spectros. Radiat. Transfer,* **46**, 412-423.

Heymsfield A. J., A. Bansemer, C. Schmitt, C. Twohy, and M. R. Poellot, 2004: Effective ice particle densities derived from aircraft data. *J. Atmos. Sci.*, **61**, 982-1003.

Li, J., H.-L. Huang, C. Y. Liu, T. J. Schmit, H. Wei, E. Weisz, L. Guan, and W. P. Menzel, 2005: Retrieval of Cloud microphysical properties from MODIS and AIRS. *J. Appl. Meteor.*, **44**, 1526-1541.

Knuteson, R. O., F. A. Best, N. C. Ciganovich, R. G. Dedecker, T. P. Dirkx, S. Ellington, W. F. Feltz, R. K. Garcia, R. A. Herbsleb, H. B. Howell, H. E. Revercomb, W. L. Smith, and J. F. Short, 2004: Atmospheric Emitted Radiance Interferometer (AERI): Part I: Instrument Design. *J. Atmos. Oceanic Technol*., **21**, 1763-1776.

Kokhanovsky, A. A., and T. Nauss, 2005: Satellite based retrieval of ice cloud properties using a semi-analytical algorithm. *J. Geophys. Res*., **110**, D19206.

Min, Q., and M. Duan, 2005: Simultaneously retrieving cloud optical depth and effective radius for optically thin clouds, *J. Geophys. Res.*, **110**, D21201.

Piironen, P., and E. W. Eloranta, 1994: Demonstration of a High-Spectral-Resolution Lidar based on a Iodine Absorption Filter. *Optics Letters*, **19**, 3, 234-236.

Revercomb, H. E., V. P. Walden, D. C. Tobin, J. Anderson, F.A. Best, N.C. Ciganovich, R.G. Dedecker, T. Dirkx, S.C. Ellington, R.K. Garcia, R. Herbsleb, R.O. Knuteson, D. LaPorte, D. McRae, and M. Werner, 1998:

Recent Results From Two New Aircraft-Based Fourier-Transform Interferometers: The Scanning High-resolution Interferometer Sounder and the NPOESS Atmospheric Sounder Testbed Interferometer. *ASSFTS Conference*, Toulouse, France.

Rothman, L. S. D. Jacquemart, A. Barbe, D. Chris Benner, M. Birk, L. R. Brown, M.R. Carleer, C. Chackerian Jr., Chance, L. H. Couderth, V. Dana, V. M. Devic J.-M. Flaudh, R. R. Gamache, A. Goldman, J.-M. Hartmannh, K. W. Jucks, A. G. Maki, J.-Y. Mandini, S. T. Massie, J. Orphal, A. Perrin, C. P. Rinsland, M. A. H. Smith, J. Tennyson, R. N. Tolchenov, R. A. Toth, J. Vander Auwera, P. Varanasi, and G. Wagner, 2005: The HITRAN 2004 molecular spectroscopic database. *J. Quant. Spectros. Radiat. Transfer*, **96**, 139-204.

Rizzi R., M. Matricardi, and F. Miskolczi, 2002: On the simulation of up-looking and down-looking high-resolution radiance spectra using two different radiative transfer models. *Appl. Opt.*, **41**, 9.

Turner, D. D., 2005: Arctic mixed-phase cloud properties from AERI-lidar observations: Algorithm and results from SHEBA, *J. Appl. Meteor.*, **44**, 427-444.

Yang, P., H. Wei, H.-L. Huang, B. A. Baum, Y. X. Hu, G. W. Kattawar, M. I. Mishchenko, and Q. Fu, 2005: Scattering and absorption property database for nonspherical ice particles in the near through far infrared database. *Appl. Opt.*, **44**, 26.